Research Square

Preprints are preliminary reports that have not undergone peer review.
They should not be considered conclusive, used to inform clinical practice,
or referenced by the media as validated information.

Three-Dimensional Anatomical Classification and Machine Learning Prediction of the P6a–Right Hepatic Vein Relationship: Surgical Implications for Laparoscopic Right Anterior Sectionectomy

haoming li
AIR FORCE MEDICAL CENTER
chengli liu
liuchengli_beijing@163.com

AIR FORCE MEDICAL CENTER
jingchen zhang
Hebei North University
hao huang
Second Affiliated Hospital of Anhui Medical University
meng pu
AIR FORCE MEDICAL CENTER
yingbo ma
AIR FORCE MEDICAL CENTER
linghong kong
AIR FORCE MEDICAL CENTER

Research Article

Keywords:

Posted Date: July 28th, 2026

DOI: https://doi.org/10.21203/rs.3.rs-10347193/v1

License: This work is licensed under a Creative Commons Attribution 4.0 International License.
Read Full License

Additional Declarations: No competing interests reported.

Version of Record: A version of this preprint was published at Surgical and Radiologic Anatomy on October 14th, 2026. See the published version at https://doi.org/10.1007/s00276-026-04016-4.

Abstract

Background: The spatial relationship between the ventral branch of segment VI portal vein (P6a) and the right hepatic vein (RHV) significantly influences the anatomical complexity of the right hepatic fissure and the surgical outcomes of laparoscopic right anterior sectionectomy (LRAS). The ventral-P6a variant is often associated with higher surgical risks, yet preoperative prediction remains challenging.

Methods: This retrospective study included 100 patients who underwent triple-phase enhanced CT of the upper abdomen. Based on three-dimensional reconstructions, P6a was classified as dorsal or ventral relative to the RHV according to its anatomical relationship. Five machine learning models—logistic regression, random forest, K-nearest neighbors, support vector machine, and XGBoost—were employed to predict P6a classification using anatomical angular and linear measurements. Model performance was evaluated using the area under the receiver operating characteristic curve (AUC) and the F1-score, and the SHAP method was applied for feature interpretation.

Results: Among the 100 patients, 59% were classified as dorsal-P6a and 41% as ventral-P6a. The ventral-P6a group exhibited a significantly smaller angle between the anterior and posterior portal branches (82.27° vs. 98.02°, P=0.003), a higher proportion with a distance of less than 5 mm from the P6a origin to the posterior branch origin (37% vs. 10%, P=0.001), and a larger RHV-inferior vena cava angle (52.23° vs. 43.97°, P=0.013). The logistic regression model demonstrated the best performance in the test set (F1-score=0.741) with minimal overfitting. The most important predictive features included the angle between the anterior and posterior portal branches, the angle of the right hepatic fissure plane, and the diameter of P6a. SHAP analysis validated the interpretability of the model.

Conclusion: A machine learning model based on three-dimensional imaging anatomical features can effectively predict the spatial classification of P6a relative to the RHV. The interpretable logistic regression model identifies key anatomical risk factors, providing a basis for preoperative risk assessment and surgical planning in LRAS, particularly for optimizing surgical strategies in high-risk patients with the ventral-P6a variant.

Introduction

In the Couinaud liver segmentation system, the right hepatic vein (RHV) lies within the right hepatic fissure, which serves as a key anatomical landmark dividing the right anterior and right posterior sections of the liver [1]. However, the RHV does not always follow the expected course along the right hepatic fissure [2]. This anatomical variation poses significant challenges to surgeons during liver resection, particularly in identifying the right hepatic fissure accurately, often leading to depth disorientation. Such disorientation may result in ischemia of the remaining liver parenchyma and difficult-to-control bile leaks, which severely impact surgical outcomes and patient recovery[3, 4].These risks are further magnified in laparoscopic right anterior sectionectomy (LRAS), a procedure involving complete resection of segments S5 and S8 and requiring simultaneous control of the confluence of the

middle hepatic vein (MHV), RHV, and inferior vena cava (IVC). LRAS is one of the most extensive liver resections in terms of resection volume [5, 6]. Therefore, precise preoperative identification of the RHV trajectory and three-dimensional configuration of the right hepatic fissure becomes a critical step in reducing the risks associated with LRAS.

The spatial relationship between the ventral branch of segment VI portal vein (P6a) and the RHV serves as a crucial key to deciphering the complexity of the right hepatic fissure. Studies have found that P6a runs dorsal to the RHV in 76% of cases (dorsal-P6a type), while in 12% it is located ventral to the RHV (ventral-P6a type)[4]. The ventral-P6a type is often associated with various anatomical variations in the region of the right hepatic fissure and the right hepatic hilum, whereas anatomical variations of the dorsal-P6a type are relatively fewer[4]. Given that the right hepatic fissure itself is not flat and the hilar anatomy is more complex in the ventral-P6a type, relying solely on two-dimensional imaging often leads to an underestimation of surgical risks for this variant.

Machine learning (ML) has recently demonstrated superior performance in predicting clinical outcomes and aiding diagnosis. Compared to traditional statistical methods, ML can effectively capture complex interactions and non-linear associations among variables, leading to its increasing application in clinical research—where outcomes often depend on intertwined influences of multiple factors[7–9]. However, despite significant and sustained progress over the past decade, ML models are often viewed as "black boxes" due to their lack of interpretability. The rise of Explainable Artificial Intelligence (XAI) methods helps address this issue. XAI employs a range of techniques to enable clinicians and researchers to understand the decision-making process and output logic of ML algorithms, thereby enhancing model transparency and promoting the acceptance and integration of artificial intelligence in clinical practice[10].

This study aims to develop an interpretable ML model using clinical data to predict the spatial position of P6a relative to the right hepatic vein. By leveraging Explainable Artificial Intelligence techniques, the model will assist clinicians in interpreting its predictions, thereby fostering a more systematic understanding of the anatomical variation characteristics of the right hepatic fissure and right hepatic hilum. This approach not only facilitates precise preoperative assessment of surgical risks but may also provide a basis for categorizing potential intraoperative challenges in laparoscopic right anterior sectionectomy (LRAS), ultimately aiding surgeons in better managing this complex procedure [11].

Methods

Study Population

This retrospective observational study included 100 patients (49 males, 51 females) who underwent triple-phase dynamic contrast-enhanced CT scans (arterial, portal venous, and delayed phases) of the upper abdomen at the Hepatobiliary Surgery Department of the Air Force Medical Center between September 2022 and December 2024. Inclusion criteria were: (1) no space-occupying lesions in the right

anterior liver parenchyma; (2) no history of hepatic surgery, interventional therapy, or radiofrequency ablation; (3) complete triple-phase CT images (arterial, portal venous, and delayed phases) with clear visualization of tertiary portal vein branches and a slice thickness ≤ 2 mm. Exclusion criteria were: (1) incomplete imaging data of tertiary portal vein branches; (2) respiratory motion artifacts affecting vasculature assessment. All CT image data were exported from the Picture Archiving and Communication System (PACS) in DICOM format. Two radiologists independently assessed the images in a blinded manner. The Hisense Computer-Assisted Surgery (CAS) system was used to reconstruct complete three-dimensional (3D) visualization models of the portal and hepatic veins. Liver segmentation was defined according to the Couinaud classification. This study was approved by the Ethics Committee of the Air Force Medical Center [Approval No.: AFMC (Research) 2024-42-PJ01].

3D Image Measurement Parameters

Based on existing literature[4], P6a refers to the ventral branch of the segment VI portal vein. Using the 3D visualization system, P6a was classified into two types according to its anatomical relationship with the right hepatic vein (RHV): if P6a ran dorsal to the RHV, it was classified as the dorsal-P6a type; if it ran ventral to the RHV, or if the main trunk of the RHV was not distributed in the S5/S6 area, it was defined as the ventral-P6a type (Fig. 1).

Based on 3D CT reconstructions, the following anatomical angles were measured: the angle between the anterior portal branch and the right or posterior portal branch (Fig. 2A), the angle between the RHV and the inferior vena cava (IVC) (Fig. 2B), and the angle between segments S6 and S7 along the course of the RHV(Fig. 2C). The frequency of cases where the distance between the origin point of P6a and the origin point of the posterior portal branch was less than 5 mm was also recorded.

Machine Learning Models

The included data were randomly split into a training set and a test set at a ratio of 7:3. Five supervised machine learning models were ultimately constructed and tested: Logistic Regression (LR), Random Forest (RF), K-Nearest Neighbors (K-NN), Support Vector Machine (SVM), and eXtreme Gradient Boosting (XGBoost). The area under the receiver operating characteristic curve (AUC), sensitivity, specificity, precision, and F1-score with their confidence intervals (CI) were calculated for both the training and test sets. AUC and F1-score were the primary metrics for model performance comparison[12, 13]. All five ML models were trained using R statistical software version 4.4.1.

Feature importance for prediction was explored by summarizing and calculating the mean values of each feature across all patients. The SHapley Additive exPlanations (SHAP) method was employed to interpret the machine learning models and determine the impact of features on the prediction outcome. The SHAP method aids in interpreting ML models at both cohort and individual patient levels [14]. The SHAP feature importance plot illustrates the global importance of each feature; a larger mean absolute SHAP value indicates higher importance of that feature for the model's prediction. The SHAP summary

plot displays the impact of each feature on the predictive model. Each point in the summary plot represents the SHAP value for a feature of a single patient, with colors ranging from red to blue indicating high to low feature values.

Statistical Analysis

Comparisons of categorical variables between groups were performed using Pearson's χ^2 test or Fisher's exact test. Differences in continuous variables between groups were analyzed using the Mann-Whitney U test (for two independent samples) or the Kruskal-Wallis H test (for multiple groups) based on data distribution characteristics. Spearman's rank correlation analysis was used to assess correlations between continuous variables. All statistical analyses were conducted using R software version 4.4.1. A significance level of $\alpha = 0.05$ (two-tailed) was set, with $P < 0.05$ considered statistically significant.

Results

Baseline Characteristics

Based on the study data, 59 patients (59%) were classified as the dorsal-P6a type, and 41 patients (41%) as the ventral-P6a type (Table 1). In 21 patients (21%), the distance between the origin of P6a and the origin of the right posterior portal branch was less than 5 mm. The diameter of P6a exceeded 3 mm in 21 patients (21%). The RHV was fully exposed on the transection plane by the virtual LRAS in 59 patients (59%).

Intergroup comparisons revealed that the angle between the anterior and posterior portal branches was significantly smaller in the ventral-P6a group than in the dorsal-P6a group (median: 82.27° vs. 98.02°, P = 0.003). The incidence of an angle less than 60° between the right anterior and right posterior portal branches was also higher in the ventral-P6a group (29% vs. 10%, P = 0.014). Furthermore, the proportion of patients with a distance of less than 5 mm between the P6a origin and the anterior/posterior portal branch origins was significantly higher in the ventral-P6a group (37% vs. 10%, P = 0.001). The incidence of a P6a diameter > 3 mm was also significantly greater in the ventral-P6a group (56% vs. 32%, P = 0.017).

Three-dimensional image analysis indicated that the angle between the RHV and the inferior vena cava (IVC) was significantly larger in the ventral-P6a group than in the dorsal-P6a group (52.23° vs. 43.97°, P = 0.013), with a higher proportion of patients having an RHV-IVC angle > 45° (71% vs. 42%, P = 0.005). Concurrently, the angle between segments S6 and S7 along the RHV was steeper (more acute) in the ventral-P6a group compared to the dorsal-P6a group (150.8° vs. 158.7°, P < 0.001).

Table 1
Anatomical and three-dimensional CT findings in the dorsal P6a group (n = 59) and ventral P6a group (n = 41).

The angle between anterior and right branch of PV	**Dorsal-P6a (N = 59)**	**Ventral-P6a (N = 41)**	**p-value**
	143.80 (129.15, 148.80)	**147.00 (133.30, 152.30)**	**0.300**
The angle between anterior and posterior branches of PV	98.02 (80.33, 108.10)	82.27 (59.04, 97.27)	0.003
The angle between anterior and posterior branches of PV < 60°	6 (10%)	12 (29%)	0.014
The length between the origin of P6a and the origin of posterior branch of portal vein < 5 mm	6 (10%)	15 (37%)	0.001
Presence of P6a of > 3 mm in diameter	19 (32%)	23 (56%)	0.017
The angle between RHV and IVC in the 3D CT image	43.97 (40.26, 54.63)	52.23 (43.96, 62.63)	0.013
The angle between RHV and IVC > 45° in the 3D CT image	25 (42%)	29 (71%)	0.005
The angle between segment VI and segment VII along the RHV in the 3D image	158.70 (152.50, 164.60)	150.80 (141.00, 156.30)	< 0.001

Model Evaluation and Interpretation

Among the machine learning models developed to predict the P6a-RHV spatial relationship in the training set, all models demonstrated favorable AUC values (RF: 0.997; XGBoost: 0.981; SVM: 0.941; LR: 0.910; KNN: 0.847) (Fig. 3 and Table 2). This metric was further employed to compare model performance in the test set. In the test set, LR and SVM exhibited the highest AUC values (SVM: 0.789; LR: 0.770). Additionally, the F1-score was used to assess model accuracy. This metric effectively evaluates model performance in the context of class-imbalanced data by considering both precision (positive predictive value) and recall (sensitivity)[12, 13]. In the test set (Table 3), the LR model achieved the highest F1-score (0.741, 95% CI: 0.574–0.914); XGBoost also attained a relatively high F1-score (0.714, 95% CI: 0.403–0.877). Among all machine learning models, the LR model obtained the highest F1-score and demonstrated the least variation between the training and test sets, indicating minimal overfitting. Consequently, the LR model was selected for all subsequent analyses.

Table 2
Evaluation of Model Performance in the Training Set

Model	AUC	Sensitivity	Specificity	Precision	F1_Score
LR	0.910 (0.839–0.961)	0.724 (0.574–0.883)	0.857 (0.773–0.947)	0.778 (0.644–0.918)	0.750 (0.595–0.874)
RF	0.997 (0.990-1.000)	0.931 (0.785–0.994)	1.000 (1.000–1.000)	1.000 (1.000–1.000)	0.964 (0.921-1.000)
KNN	0.847 (0.777–0.931)	0.690 (0.509–0.903)	0.857 (0.770–0.954)	0.769 (0.574–0.912)	0.727 (0.552–0.834)
SVM	0.941 (0.861–0.975)	0.241 (0.107–0.437)	0.071 (0.000-0.153)	0.152 (0.069–0.258)	0.187 (0.058–0.289)
XGBoost	0.981 (0.948-1.000)	0.931 (0.816-1.000)	0.952 (0.903-1.000)	0.931 (0.847-1.000)	0.931 (0.834–0.981)

K-NN: K-nearest neighbors algorithm; LR: logistic regression; RF: random forest; SVM: support vector machine; XGBoost: eXtreme Gradient Boosting algorithm.

Table 3
Evaluation of Model Performance in the Test Set

Model	AUC	Sensitivity	Specificity	Precision	F1_Score
LR	0.770 (0.500-0.895)	0.833 (0.603-1.000)	0.706 (0.531–0.881)	0.667 (0.418–0.855)	0.741 (0.574–0.914)
RF	0.696 (0.581–0.917)	0.667 (0.427–0.885)	0.647 (0.464–0.830)	0.571 (0.235–0.844)	0.615 (0.400-0.741)
KNN	0.735 (0.532–0.893)	0.667 (0.500-0.983)	0.765 (0.616–0.937)	0.667 (0.452–0.875)	0.667 (0.412–0.810)
SVM	0.789 (0.501–0.956)	0.333 (0.016–0.616)	0.235 (0.066–0.470)	0.235 (0.060–0.443)	0.276 (0.083–0.504)
XGBoost	0.662 (0.535–0.836)	0.833 (0.648-1.000)	0.647 (0.438–0.845)	0.625 (0.444–0.854)	0.714 (0.403–0.877)

K-NN: K-nearest neighbors algorithm; LR: logistic regression; RF: random forest; SVM: support vector machine; XGBoost: eXtreme Gradient Boosting algorithm.

The results of the feature importance analysis for the LR model are shown in Fig. 4A. The evaluated features were ranked in descending order of their mean importance values to illustrate their impact on outcome prediction. The top five important features were: the angle between the anterior and posterior portal branches, the angle of the right hepatic fissure plane, the distance from the P6a origin to the posterior portal branch origin, the indicator for a distance from the P6a origin to the posterior portal branch origin of less than 5 mm, and the diameter of P6a. The summary plot of mean feature importance for the LR model demonstrates the influence of each element on the predictive model. Based on the predictive model, a higher mean importance value for a feature indicates a greater likelihood of P6a running dorsal to the right hepatic vein.Furthermore, Fig. 4B displays the impact of each feature's SHAP value on outcome prediction. It illustrates that a larger angle of the right hepatic fissure plane is associated with a higher probability of P6a coursing dorsal to the right hepatic vein.

Discussion

Among the five machine learning prediction models evaluated, the Logistic Regression (LR) model demonstrated the best performance. We further employed the SHAP method to interpret the LR model, identifying the angle of the right hepatic fissure and the angle between the right anterior and right posterior portal branches as the features with the highest predictive importance. Furthermore, to elucidate the prediction mechanism of the Random Forest (RF) model, we utilized SHAP summary plots and dependence plots to identify key predictors for the spatial relationship of P6a relative to the RHV within the cohort.

The Glissonian sheath technique has established its value in laparoscopic anatomical hepatectomy, especially in right anterior sectionectomy; however, the application of the hepatic fissure approach in laparoscopic right anterior sectionectomy (LRAS) has declined in recent years [12, 13]. Anatomical studies have shown that in patients with ventral-type P6a, the P6a branch mostly originates from the ventral side of the portal vein bifurcation into the anterior and posterior branches, resulting in a narrower “APR triangle” [14] formed by the right anterior portal branch, right posterior portal branch, and right hepatic vein (RHV) compared with patients with dorsal-type P6a (37% vs. 10%). In LRAS, due to the limited angle for instrument manipulation, special care should be taken to avoid injury to the P6a or the confluence of the right anterior Glissonian pedicle when using the pedicle dissection method. For patients with ventral-type P6a, to ensure the safety of the Glissonian sheath approach, it is recommended to fully dissect the right anterior Glissonian pedicle distally to create sufficient operating space.

During laparoscopic resection of tumors in Couinaud segment VIII, the lesion is often located in a three-dimensionally complex anatomical region: deeply situated between the middle hepatic vein (MHV) and the right hepatic vein (RHV), and adjacent to the stereotactic triangle formed by the inferior vena cava (IVC) and the right anterior Glissonian pedicle. The tumor in this location is deep, and the laparoscopic

view often fails to fully expose the surgical field. When performing retrograde dissection of the root of the right hepatic vein, interference from the right posterior hepatic vein may occur. The present study found that patients with ventral-type P6a have a larger angle between the RHV and the IVC. During laparoscopic dissection of the root of the right hepatic vein [15, 16], especially in patients with ventral-type P6a, the surgeon may inadvertently injure a sizable right posterior hepatic vein, which could lead to ischemia of the remnant liver and varying degrees of functional impairment [17].

Currently, the determination of intersegmental planes in anatomical hepatectomy is typically achieved by portal vein staining with indocyanine green or selective occlusion of the corresponding portal pedicles. Liver resection based on portal territory is more consistent with oncological requirements. However, in many cases, exposure of the main hepatic veins remains an important landmark for identifying the transection plane during anatomical hepatectomy [19–21]. Especially when fluorescence staining techniques are not yet widely available, the hepatic vein-guided approach—using the main trunk of the hepatic vein as a guide to identify the intersegmental plane—is still the preferred method for most liver surgeons and has been shown to effectively reduce the incidence of perioperative complications [22]. Because the hepatic vein has a thin wall and numerous branches, it is highly susceptible to injury and bleeding; therefore, inadvertent injury and hemorrhage from hepatic vein branches during surgery remain a common and challenging issue. As the traditional demarcation between the right anterior and right posterior sections, the right hepatic vein (RHV) plays a crucial guiding role in surgeries involving this region. The present study showed that the bending angle of the right crossing plane in patients with dorsal-type P6a is significantly larger than that in patients with ventral-type P6a, i.e., the right crossing plane is flatter in dorsal-type patients. A flat right crossing plane can serve as a reliable intraoperative anatomical landmark (Fig. 2C–2D). In contrast, in patients with ventral-type P6a, the RHV runs more dorsally, resulting in a lower intraoperative exposure rate of the RHV and a steeply sloping S6 region. In such cases, intraoperative ultrasound guidance is required to complete the parenchymal transection between S5 and S6 in areas where the RHV is not visible.

While this study successfully predicted the spatial classification of P6a relative to the right hepatic vein using a machine learning approach and proposed optimized strategies for LRAS, several limitations must be acknowledged. First, the relatively small sample size (n = 100) and the single-center retrospective design may introduce selection bias, limiting the generalizability of the findings. Second, prospective clinical studies based on this classification strategy have not yet been conducted; therefore, an evidence-based medical association between this classification system and the rates of surgical complications, the extent of functional liver preservation, or long-term patient survival benefits remains to be established. Future studies should further explore the following aspects: validating the anatomical universality and clinical stability of this classification standard through multicenter, large-sample cohorts; designing randomized controlled trials guided by this classification; and integrating this system with novel technologies such as robot-assisted surgery and augmented reality navigation. These efforts should systematically evaluate its clinical application value from multiple dimensions, including surgical safety, functional protection, and oncological outcomes

Conclusions

Machine learning models can effectively identify the spatial classification of P6a relative to the right hepatic vein based on readily available clinical data. By employing SHAP methods to interpret the predictions, an interpretable model suitable for clinical decision-making was constructed. In laparoscopic right anterior sectionectomy, this classification prediction holds clear anatomical and operative significance. For patients with the ventral-P6a type, challenges are significantly increased due to a narrow APR triangle, insufficient exposure of the right hepatic vein, and a steep angle between segments S7 and S6, which complicates the Glissonian approach and anatomical exposure. In contrast, for patients with the dorsal-P6a type, the flatter liver transection surface, complete exposure of the right hepatic vein, and well-defined anatomical landmarks facilitate more precise and safer surgical procedures.

Declarations

Conflict of Interest

All authors declare that they have no conflict of interest.

Authors' Contributions Haoming Li: Performed the research, analyzed the data, and wrote the article. Meng Pu: Collected the data. Yingbo Ma: Analyzed the data and critically reviewed the intellectual content of the article. Chengli Liu: Designed the experiment, performed the research, critically reviewed the intellectual content of the article, and provided guidance.

Compliance with Ethical Standards

Funding

Disclosure of potential conflicts of interest

The authors declare that they have no relevant financial or non-financial conflicts of interest to disclose.

Research involving human participants and/or animals

This retrospective study involving human participants was approved by the Ethics Committee of the Air Force Medical Center (Approval No. AFMC [Research] 2024-42-PJ02). The study was conducted in accordance with the ethical standards of the institutional research committee and with the Declaration of Helsinki and its subsequent amendments. This study did not involve animals.

Informed consent

Written informed consent was obtained from all individual participants included in the study.

Author Contribution

Haoming Li: Performed the research, analyzed the data, and wrote the article. Meng Pu: Collected the data. Yingbo Ma: Analyzed the data and critically reviewed the intellectual content of the article. Chengli Liu: Designed the experiment, performed the research, critically reviewed the intellectual content of the article, and provided guidance.

Data Availability

The datasets generated and/or analyzed during the current study are not publicly available due to patient privacy and ethical restrictions but are available from the corresponding author on reasonable request, subject to approval by the relevant institutional ethics committee.

References

1. BISMUTH H (1982) Surgical anatomy and anatomical surgery of the liver [J]. World J Surg 6(1):3–9
2. ZHANG F, XU Z (2022) A comprehensive framework of the right posterior section for tailored anatomical liver resection based on three-dimensional simulation system [J]. Ann Transl Med 10(16):852
3. SATO F, IGAMI T, EBATA T et al (2014) A study of the right intersectional plane (right portal scissura) of the liver based on virtual left hepatic trisectionectomy [J]. World J Surg 38(12):3181–3185
4. YAMAMOTO Y, SUGIURA T, OKAMURA Y et al (2017) The Pitfalls of Left Trisectionectomy or Central Bisectionectomy for Biliary Cancer: Anatomical Classification Based on the Ventral Branches of Segment VI Portal Vein Relative to the Right Hepatic Vein [J]. J Gastrointest Surg 21(9):1453–1462
5. CHEN H W, WANG F J, LI JY et al (2019) Extra-Glissonian Approach for Laparoscopic Liver Right Anterior Sectionectomy [J]. JSLS, 23(2)
6. IDE T, ITO K, TANAKA T et al (2022) The short-term outcomes of laparoscopic right anterior sectionectomy: A comparison with the open procedure [J]. Asian J Surg 45(10):2129–2130
7. SHI H, YANG D, TANG K et al (2022) Explainable machine learning model for predicting the occurrence of postoperative malnutrition in children with congenital heart disease [J]. Clin Nutr 41(1):202–210
8. STEVENS L M, MORTAZAVI B J DEORC et al (2020) Recommendations for Reporting Machine Learning Analyses in Clinical Research [J]. Circ Cardiovasc Qual Outcomes 13(10):e006556
9. CHUNG H, KO Y, LEE I S et al (2023) Prognostic artificial intelligence model to predict 5 year survival at 1 year after gastric cancer surgery based on nutrition and body morphometry [J]. J Cachexia Sarcopenia Muscle 14(2):847–859

10. SAEED W O C (2023) Explainable AI (XAI): a systematic meta-survey of current challenges and future opportunities. [J]. KnowlBased Syst : 263
11. CHEN J, ZHANG Z, ZHOU R et al (2022) The APR triangle: A practical zone in the Glissonean approach to laparoscopic anatomical right hepatectomy [J]. Iliver 1(3):176–180
12. MAKUUCHI M, HASEGAWA H (1985) Ultrasonically guided subsegmentectomy [J]. Surg Gynecol Obstet 161(4):346–350
13. CHANG W, CHEN Y, ZHOU S et al (2023) Anatomical resection improves relapse-free survival in colorectal live r metastases in patients with KRAS/NRAS/BRAF mutations or right-sided colon cancer: a retrospective cohort study [J]. Int J Surg 109(10):3070–3077
14. Wang CJ, Liang X et al (2022) Theory and technical practice of portal territory-based anatomical hepatectomy for hepatocellular carcinoma. Chin J Dig Surg 21(5):591–597
15. UENO M, IIDA H, KOMEDA K et al (2022) Dorsal vs ventral approach to the middlehepatic vein during laparosco pic left hemihepatectomy: multicenter retrospective observational study [J]. Surg Endosc 36(9):6464–6472
16. SAKAMOTO K, OGAWA K, TAMURA K et al (2024) Dorsal approach in laparoscopicextended left hemi-hepatectomy: A case series [J]. Med (Baltim) 103(9):e37336
17. Cawich SO, Naraynsingh V, Pearce NW et al (2021) Surgical relevance of anatomic variations ofthe right hepatic vein [J]. World J Transplantation 11(6):231–243
18. Aoki T, Koizumi T, Mansour DA et al Ultrasound-guided pre-operative positive percutaneous indocyanine green fluorescencestaining for laparoscopic anatomical liver resection □. J Am CollSurg,2020,230(3):e7-e12. DO: 10.1016/j.jamcollsurg.2019.11.004
19. 0giso S, Seo S, Okumura S et al (2019) Laparoscopic left lateral sec-tionectomy using the extrahepatic glissonean approach: a secureoption for achieving a negative margin for lesions with ductal exten-sion[J]. Ann Surg Oncol 26(6):1858. 10. 1245/s10434-019-07298-8
20. Berardi G, Igarashi K, Li CJ et al (2021) Parenchymal sparing anatomi-cal liver resections with full laparoscopic approach : description oftechnique and short-term results[J]. Ann Surg 273(4):785–791. 10.1097/SLA.0000000000003575
21. Liao KX, Cao L, Huang D et al (2020) Clinical study of laparoscopic hepatic vein-guided anatomical hepatectomy for hepatocellular carcinoma. Chin J Hepatobiliary Surg 26(5):339–344. 10.3760/cma.j.cn113884-20191122-00381

Figures

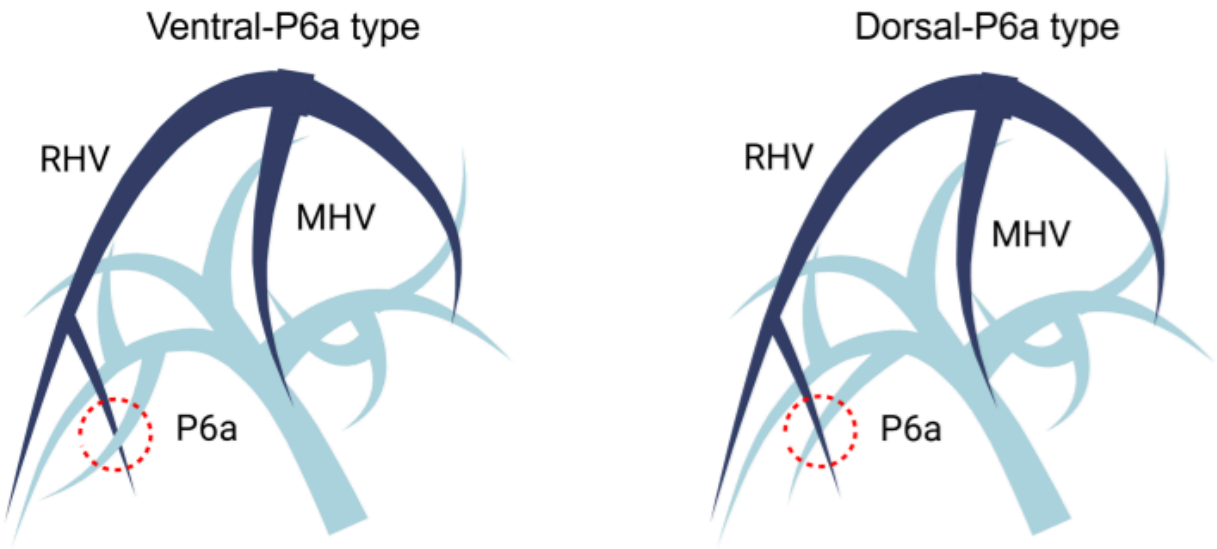


Figure 1

shows the Ventral-P6a type on the left and the Dorsal-P6a type on the right

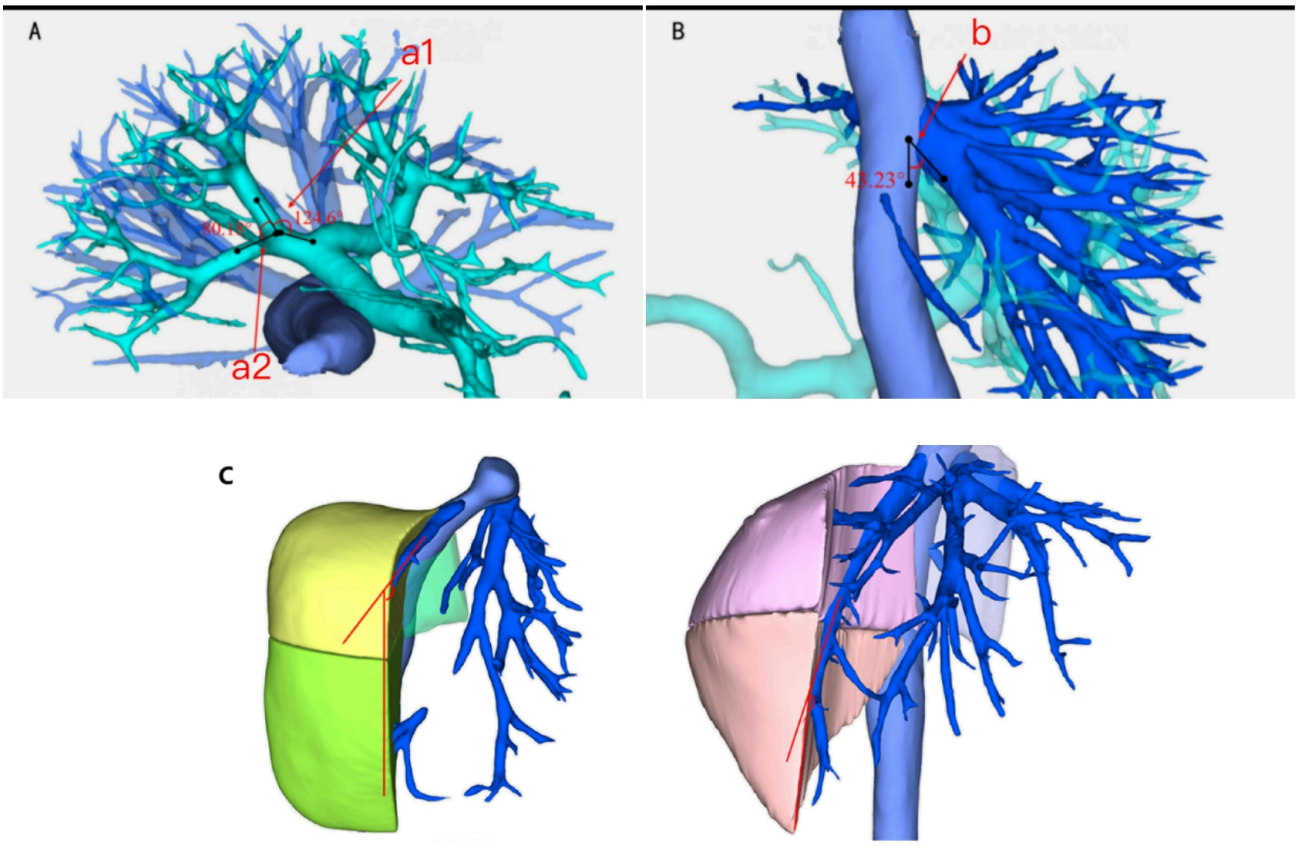


Figure 2

Left panel (A): a1: The angle between the anterior and right branches of the portal vein; a2: the angle between the anterior and posterior branches of the portal vein. Right panel (B): b: The angle between the right hepatic vein and the inferior vena cava on 3D CT imaging.Right panel (C): the angle between segments S6 and S7 along the course of the RHV

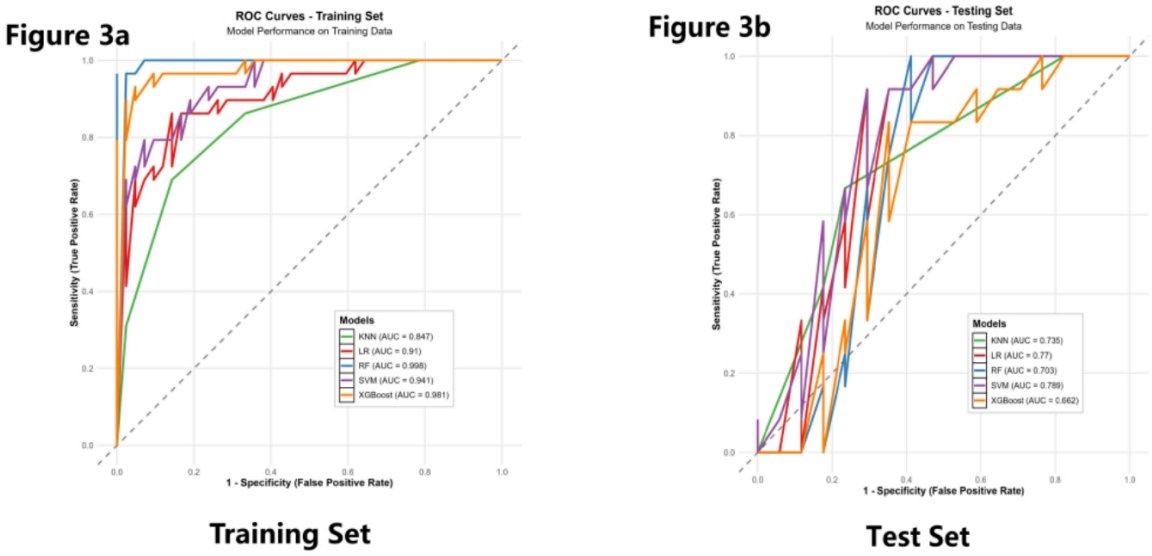


Figure 3

Receiver operating characteristic (ROC) curves showing the performance of machine learning models in predicting the spatial position of P6a relative to the right hepatic vein, based on the (A) training and (B) test datasets. K-NN: K-nearest neighbors; LR: logistic regression; RF: random forest; SVM: support vector machine; XGBoost: eXtreme Gradient Boosting.

Figure 4a

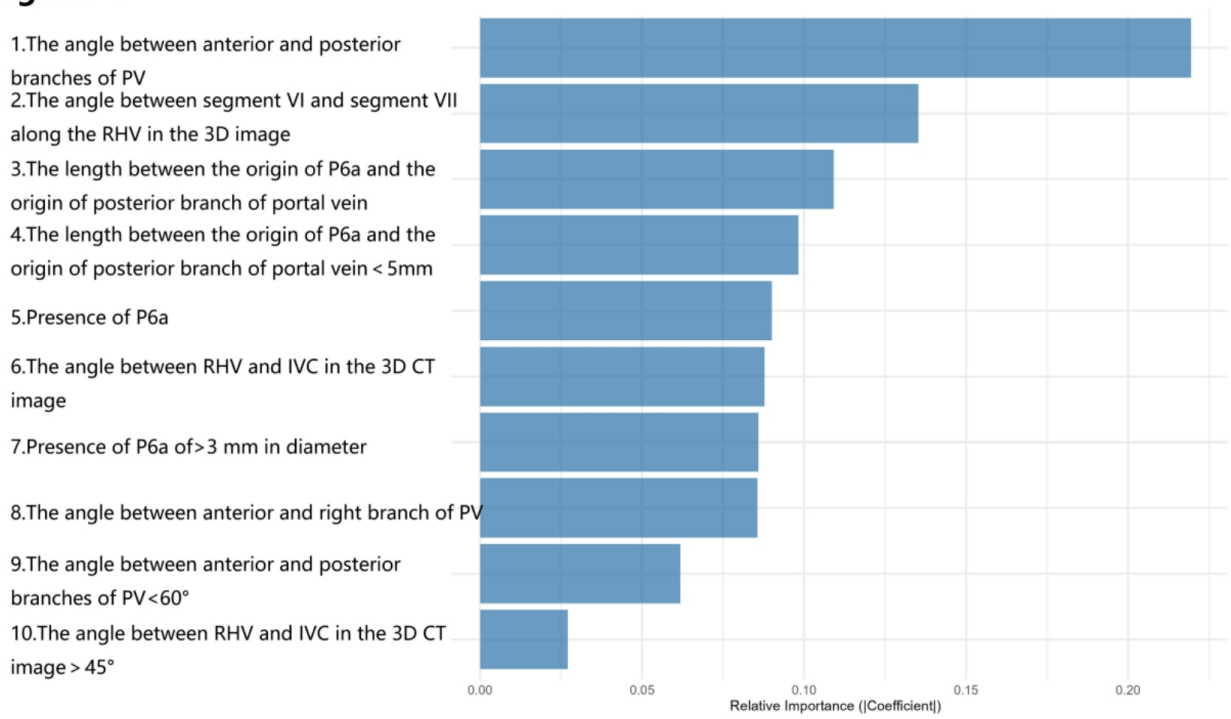


Figure 4b

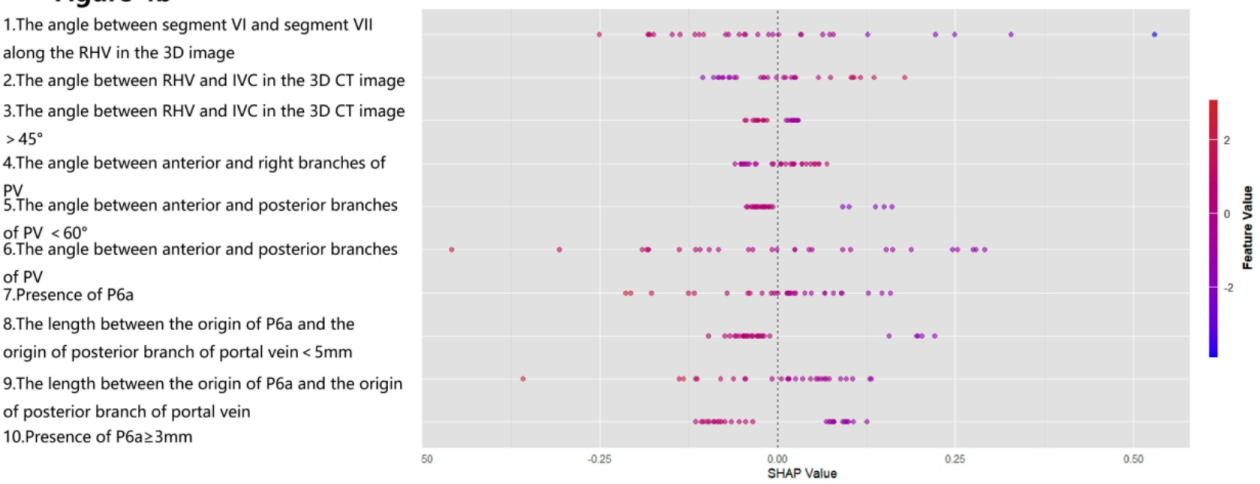


Figure 4

a shows the mean values of each feature for the LR model, and **b** presents the SHAP summary plot.